Telecorrelation of the 500 hPa Polar Circulation and El Nino / SO with the Temperature Fields in China

Shi Neng (施 能)
Nanjing Institute of Meteorology, Nanjing 210044
and *Luo Boliang* (罗伯良)
Meteorological Observatory of Hunan Province
Received June 14, 1990; revised December 9, 1990

ABSTRACT

By using the monthly data from 1951 through 1984, empirical orthogonal expansion is performed for the 500 hPa geopotential height north of 65°N and the canonical fields are clustered by fuzzy classification. It is noted that both the mean monthly polar vortex fields and the large-scale anomaly fields fall into three regimes, with those of the January mean field and th April anomaly field having characteristic features. In addition, the relationship between the time weigthing coefficients of the canonical fields and El Nino / SO is examined, showing significant anomalies in the large-scale polar anomaly fields during April and October of the year when El Nino occurs. These polar circulation anomalies have considerably influenced the temperature fields in China during April and October. Thus, we may conclude that this is one of the most important reasons for a relatively cool April and a warm October in China during the El Nino year.

1. INTRODUCTION

There exists a strong cyclonic circulation system in the NH circumpolar area, whose intensity, central position and scope are bound to exert an important impact on the long-range variation of the whole atmospheric circulation, weather regimes and sea-air interaction. To this end, considerable studies have been conducted on the relationship between the polar vortex and the weather-climate regime. However, much attention has been paid only to the extratropics (Chen, 1989), and up to now no published evidence has been shown concerning the telecorrelation between the polar vortex and the equatorical Pacific El Nino / SO.

Quite a few approaches have been proposed for the expression of the polar vortex (Dong, et al., 1987). Nevertheless, Objective and quantitative expression of the intensity and regime of the polar height field remains a problem to be solved. Dong, et al. (1987) first tried to employ the empirical orthonogal function (EOF) expansion to represent the 500 hPa polar height, However, it should be noted that in the above studies the EOF expansion was only done for the secular mean fields from January through December, and the canonical fields thus obtained can, in fact, apply only to the restoration of the secular mean fields. If the height field in a certain month of a year is to be expanded as the superposition of a canonical field, a data matrix should be made up of the monthly mean height field in that month, i.e., to expand it month by month. Such expansion is performed herein, obtaining different monthly canonical fields and annual time coefficients. These canonical fields can be classified to investigate the monthly mean fields and anomaly fields of the polar vortex, or the time coefficients of the monthly canonical fields and the eigenvalues of the El Nino / SO can be used to reflect the telecorrelation. Thus synoptic analysis and interpretation can be done of the results.

II. PRINCIPLES AND CALCULATION METHODS

1. *Calculation Methods*

Suppose that the height field in a given month is $\mathbf{X} = (\mathbf{x_{ij}})$, $\mathbf{i} = 1,2,...,\mathbf{m}$, where m is the space point, $\mathbf{j} = 1, 2,..., \mathbf{n}$, n is the yearly time point, and x_{ij} is the value of the height in that month at the i–th point during the j–th year. Since m is greater than n, time and space should be transformed before calculation, i.e., to determine the eigenvalue λ_j and eigenvector $\mathbf{U_i}$ of the n–order symmetric $A = X^T \cdot X$ and then transform them into the eigenvector V_j of $X \cdot X^T$. Thus we have

$$_m X_n = {}_m V_n Z_n \tag{1}$$

$$V_j = \frac{X \cdot U_j}{\sqrt{\lambda_j}} , \tag{2}$$

where V_j is the m–dimensional vector, $V_i = (v_{ik}), Z = (z_{kj}), i = 1,2,...,m, j = 1,2,...,n$, $k = 1,2,...,n$. Here, v_{kj} denotes the k–th component of the eigenvector V_i corresponding to the eigenvector λ_i and z_{kj} is the j–th time coefficient of the eigenvector V_k corresponding to the eigenvalue λ_k. Then Eq. (1) can be written as

$$x_{ij} = \sum_{k=1}^{n} v_{ki} \cdot z_{kj} \tag{3}$$

$$x_j = \sum_{k=1}^{n} v_k \cdot z_{kj} , \tag{4}$$

Where Eq. (4) denotes the field at any time and x_j the linear superposition of the canonical fields V_k in terms of the time weighting coefficient z_{kj}.

2. *Data and Expansion Results*

The 1951–1984 500 hPa height field data at 61 points in the NH polar area are expanded, thus we have $m = 61$ and $n = 34$. The 61 points are: 0°, 90°E, 180°, 90°W along 85°N; nine points along 80°N, 1 point every 40 longitudinal degrees from 30°E to 10°W; 12 points along 75°N, 1 point every 30 longitudinal degrees from 40°E to 10°E: 18 points along 70°N, 1 point every 20 longitudinal degrees from 10°E to 10°W; and 18 points along 65°N, 1 point every 20 longitudinal degrees from 5°E to 15°W. The expansion is conducted month by month. Table 1. shows the monthly accumulated percentages of the first 5 eigenvectors in the total variance.

Table 1. The Accumulated Percentages of the First Five Eigenvectors When the EOF Expansion of the 500 hPa Polar Height Field is Conducted

Vectors	Jan.	Feb.	Mar.	Apr.	May	Jun.	Jul.	Aug.	Sep.	Oct.	Nov.	Dec.
1st	84.6	83.8	89.5	96.8	98.8	99.2	99.5	99.3	98.9	96.5	92.5	89.9
2nd	89.1	88.6	93.8	97.6	99.1	99.4	99.6	99.5	99.1	97.6	95.0	90.4
3rd	92.5	93.1	96.0	98.2	99.4	99.5	99.7	99.6	99.3	98.4	96.5	93.5
4th	95.4	95.1	97.0	98.7	99.5	99.6	99.8	99.7	99.5	98.8	97.4	95.6
5th	96.8	96.5	98.0	99.0	99.7	99.7	99.8	99.8	99.6	99.1	98.1	96.7

Table 1 shows that the first eigenvector in each month accounts for 83.1% in the total variance and the accumulated variance of the first three ones amounts to over 92%, in which only the first one in April–October accounts for 96% of the total variance. Generally, the

monthly mean characteristics of the polar circulation can be well expressed by taking three eigenvectors. Table 1 also suggests that the first canonical field in the winter months contributes less than it does in the summer months, which agrees with the actual conditions of the polar circulation.

3. *The Regimes and Clustered Classification of the Polar Vortex Eigenvector Field*

The monthly eigenvector chart and the yearly time coefficient series have been obtained through the above expansion, but owing to the limited space, we can't show all th charts herein. However, it is of interest to give a brief account of the main regime features of the first and second eigenvector fields. Shi (1988) has pointed out that if the observational data for the polar height are taken as matrix X the first eigenvector indicates the secular mean field for the month and the second the large–scale anomaly field.

1) The first eigenvector chart shows the circles with the polar area as the low center for every month, but the locality and regimes of the lowest points differ from month to month. The chart shows that in the months from December to February the lowest point is slightly inclined to the western Hemisphere with its position at 90°–80°W. Starting from March the lowest point retreats to the eastern Hemisphere and by June–August it is found exactly at the center of the polar region, forming a circle. With the similar coefficients calculated for each other, the first eigenvectors of the twelve months (each vector has 61 dimensions) are clustered by fuzzy classification, thus obtaining a cluster chart (Fig. omitted). Results show that the monthly mean circulations can be classified into three regimes, i.e., in January, April–October, and the remaining months, respectively. Since the first canonical field in January is a Low–value area in the form of a strip near 90°W–90°E with its center in the western Hemisphere, the regime in this month is more characteristic, thus sorted out as a single regime and classified finally.

Table 2. The Mean Values (MV) of the Time Coefficients of the First Eigenvectors and Their Mean Square Deviations (MSD)

Vectors	Jan.	Feb.	Mar.	Apr.	May	Jun.	Jul.	Aug.	Sep.	Oct.	Nov.	Dec.
Mv	686.1	773.6	840.3	1178.7	1724.1	2186.0	2490.5	2332.3	1845.1	1265.3	902.9	693.1
MSD	170.1	120.1	140.7	108.5	1130.0	79.0	72.4	92.1	89.9	107.0	119.3	138.3

It is seen from Table 2 that the mean value increases from winter months to summer months, with its maximum appearing in July and minimum in January, suggesting that the polar height increases from winter to summer; and the opposite is true for the mean square deviation, with its maximum in January and minimum in July, This shows that the annual variation of the monthly mean conditions of the vortex is the greatest in January and the smallest in July.

2) The second eigenvector chart shows the large–scale anomaly field in the polar area. Two basic regimes are observed: one in October, November and December, negative in the eastern Hemisphere and positive in the western, and the other in February, July and August, positive in the eastern Hemisphere and negative in the western. For those in the remaining months, they vary in between, each having its own characteristic features. Fuzzy classification suggests that if the similarity level is properly relaxed, they can also be sorted out into three regimes, i.e., in April, October–January, and the remaining months, with the anomaly field in April being the most characteristic (see Fig. 1). As will be noted later, the time coefficients of

such anomaly fields in the El Nino year siginificantly small.

III. TELECORRELATION BETWEEN THE POLAR CIRCULATION AND EL NINO / SO

1. *The Telecorrelation Facts*

El Nino occurs in the equatorial eastern Pacific and is characterized by the anomaly of the warm sea water. During its occurrence abnormal global atmospheric circulation and weather–climate are observed. In this work, an analysis is made of the telecorrelation between the El Nino year and the polar circulation from the secular mean conditions rather than a case study of the polar circulation anomaly in a single El Nino year. Obviously, the telecorrelation employed here, in a probability sense, also exists in a single El Nino year. Table 3 lists the selected El Nino and anti–El years (Wang, 1985;Shi, 1989 and Li, 1986). Besides, the yearly values of the first SO principal component that reflect the intensity of the SO year are also taken as the eigenvectors for calculating the telecorrelation.

Table 3. The El Nino and Anti–El Nino Years from 1551 to 1984

El Nino yr.	1951,	1953,	1957,	1963,	1965,	1969,	1972,	1976,	1982,	1983
Anti–El Nino yr.	1954,	1955,	1964,	1967,	1970,	1973,	1975			

Table 4 lists the correlation coefficients between the time coefficients of the lst–3rd canonical fields in the polar height field and the first principal components of the SO indexes (SOI), with only a sign given when the absolute value is smaller than 0.1.

Table 4. *The Correlation Coefficients between the lst–3rd Time Coefficients of the Polar Height Field by EOF* Expansion and the First Principal Component of the SOI

Co.	Jan.	Feb.	Mar.	Apr.	May	Jun.	Jul.	Aug.	Sep.	Oct.	Nov.	Dec.
lst	−0.32*	−	0.11	0.13	−0.23	−	−0.18	−0.12	−	−	−	−
2nd	0.17	0.14	+	0.47**	+	−	0.23	+	−	0.41**	+	−
3rd	−	−0.16	−	−	0.27	0.12	−	0.24	0.24	+	0.11	+

Table 5 gives the values of the first time coefficients in January, and the second ones in April and October in the El Nino and anti–El Nino years as well as their means and mean square deviations.

Table 5. The Values Taken From the Three Time Coefficients in the El Nino and Anti–El Nino Years by EOF Expansion of the Polar Height Field

El Nino year	Jan lst co.	Apr. 2nd co.	Oct. 2nd co.	Anti–El–Nino year	Jan lst co.	Apr. 2nd co.	Oct. 2nd co.
1951	541.4	−93.2	−103.1	1955	625.8	−92.8	305.2
1953	686.6	−193.8	−177.5	1954	789.1	16.5	−171.3
1957	547.1	−44.2	−123.3	1964	406.8	59.8	−51.3
1963	913.9	−46.0	−106.3	1967	560.0	−160.5	1.7
1965	679.0	−64.1	67.9	1970	880.3	0.3	81.1
1969	960.1	34.8	−97.4	1973	469.4	68.4	212.5
1972	511.1	−49.9	−85.0	1975	365.1	−52.2	160.7
1976	555.3	−99.8	−99.4				
1982	653.0	−92.3	3.2				
1983	479.0	−33.8	−56.0				
Mean	652.8	−68.2	−77.0	Mean	585.2	−22.9	76.9
MSD	157.4	55.9	65.3	MSD	179.1	77.4	151.8

Table 4 suggests that the correlation coefficients of the first coefficients of the polar height and the SOI in January have approached the significance level of 0,05, and those of the second time coefficients and the SOI in April and October have approached the significance level of 0.01. And Table 5 shows that the difference in the mean values of the three time coefficients in the El Nino and anti–El Nino years are significant, with their significance approaching and exceeding 0.05 respectively.

2. *The Polar Circulation Anomaly and El Nino / SO in April and October*

As has been mentioned above, the first coefficients in January and the second coefficients in April and October are closely related to El Nino / SO. Owing to the fact that the correlation between the polar circulation and El Nino / SO is significantly higher, a more detailed analysis is to be made of the relation–ship between them.

(1) *The polar circulation in April*

Fig.1 shows the second eigenvector in April by the EOF expansion of the polar height field.

It is seen from Fig.1 that the vector space is of two–wave type, with the low–value center situated in the polar area of northern Darts of Europe and Canada and the high–value in the polar area. As the time coefficient of the second eigenvector in April of the El Nino year is significantly small (see Table 5), the anomaly distribution pattern north of 60°N is basically opposite to the regime of the eigenvector field on the composite 500 hPa anomaly chart in April, as shown in Fig.2. Three low–value centers are observed in the Arctic Ocean, eastern Siberia and the North Atlantic and a high–value center exists over the northern parts of Eurrasia and Canada. In the circulation regime both the blocking high over the Ural area and Canada and the huge trough along the east coasts of the two continents are persistently abnormal, thus favorable to the steady transportation of cold air to the mid–latitudes, especiallyto East Asia, thus causing an increase of cold air activities over the area.

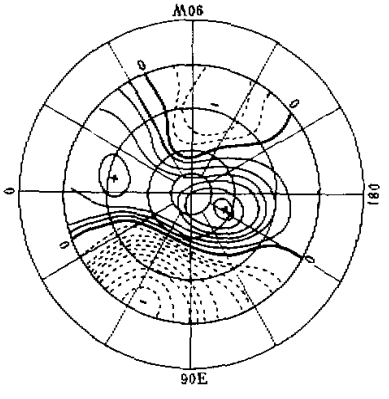

Fig.1. The second canonical field in April.

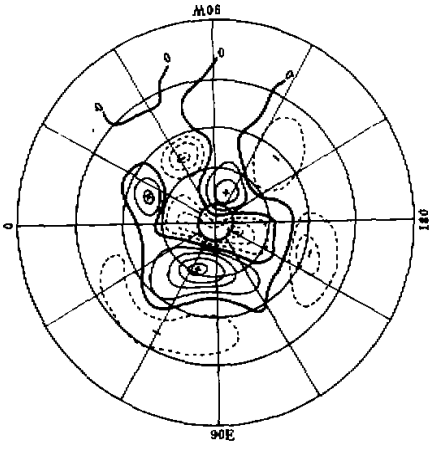

Fig.2. The composite 500 hPa anomaly chart in April of the El Nino year. Unit: geopotential 10m.

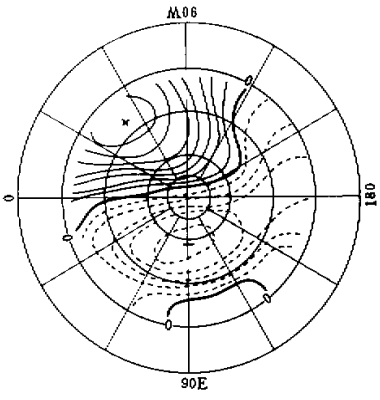

Fig.3. The second eigenvector field in October.

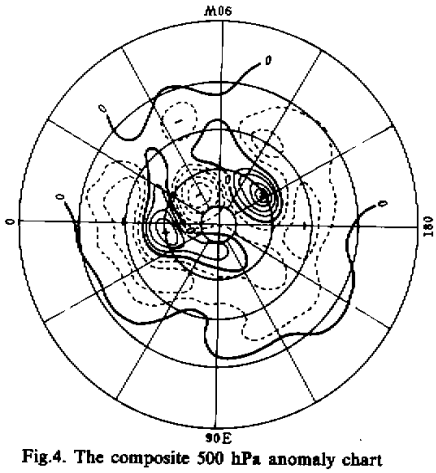

Fig.4. The composite 500 hPa anomaly chart in October of the El Nino year. Unit: Geopotential 10m.

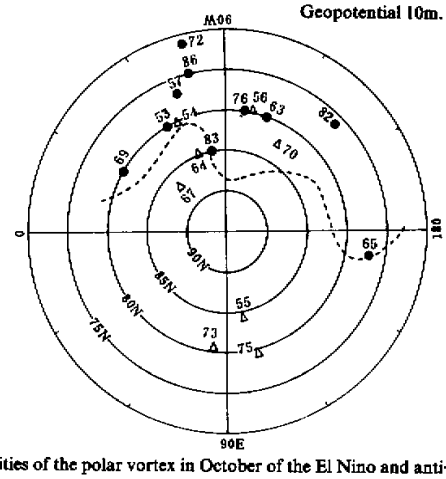

Fig.5. The localities of the polar vortex in October of the El Nino and anti-El years (1952–1986).

(2) *The polar circulation in October*

Fig.3 portrays the second eigenvector field in October by the EOF expansion of the polar height field. The spatial distribution is of one-wave type, with the height in the western Hemisphere, especially in the area of 0°–90°W, obviously higher and that in the eastern Hemisphere lower. Due to the relatively smaller weighting coefficients in the El Nino year (see Table 5), the height of the polar area in the western Hemisphere will be on the low side and that in the eastern Hemisphere on the high side in the El Nino year. The composite anomaly chart in October of the El Nino year has confirmed this (see Fig.4).

Because of the low height in the western Hemisphere, especially in the area of 0°–90°W in October of the El Nino year, the polar vortex center is inclined to the western Hemisphere. Fig.5 shows the localities of the polar vortex in the El Nino and anti-El Nino years of 1952–1986. Two features are observed, i.e., in the El Nino years, the polar vortex centers are

situated in the western Hemisphere, from 170°E to 30°E and north of 85°N, and in the anti-El Nino years they are found in the eastern Hemisphere (1955, 1973 and 1975) or in the wesiern Hemisphere but north of 82°N (1964, 1967 and 1970) with an exception only in 1954.

IV. THE TEMPERATURE FIELD IN CHINA IN APRIL AND OCTOBER AND EL NINO / SO

So far we have examined the telecorrelation between El Nino and the 500 hPa height fields in the polar area during April and October. Now we shall come to the anomaly of the temperature fields.

1. *Frequent Occurrences of Cold Waves and Severe Cold Air in China during April*

As has been mentioned earlier, the persistent anomalies of the blocking high over the Ural area and Canada and the huge trough along the east coast of the two continents in April of the El Nino year is favorable to the movement of the polar cold air to East Asia. Table 6 gives the occurrences of cold wave and severe cold air over China in April (Shi, et al., 1989).

Table 6. The Occurrence Frequency of Cold Wave and Severe Cold air over China in April from 1951 to 1984

El Nino year	Times	Normal year	Times	Anti-El Nino Year	Times
1951	–	1952	2	1954	2
1953	1	1956	1	1955	2
1957	1	1958	1	1964	1
1963	2	1959	1	1967	1
1965	3	1960	1	1970	0
1969	3	1961	2	1973	0
1972	3	1962	2	1975	0
1976	1	1966	2		
1982	2	1968	2		
1983	2	1971	1		
		1974	0		
		1977	1		
		1978	2		
		1979	2		
		1980	3		
		1981	0		
		1984	0		
Average	2.0	Average	23 / 17	Average	0.85

It is seen from Table 6 that there are observed more cold waves and severe cold air flows than normal in April of the El Nino year (twice on the average) but less in the anti-El Nino year (less than once on the average). If we look directly into the temperature fields, the results will be more obvious. Table 7 shows the correlation coefficients between the mean temperatures in April and October at 38 weather stations all over the country and the first SO principal components.

It is seen from Table 7 that of the 38 April correlation coefficients 4 reach the significance level of 0.05, mostly distributed south of the Changjiang River. However, all the 38 correlation coefficients are positive, indicating that in April of the weak SO years the temperatures are on the low side. In addition, the mean value differences (the mean values in the El Nino years minus those in the anti-El Nino years) at the 38 stations are also calculated, and they are all negative, suggesting that the temperatures in April of the El Nino year are in the main on the low side.

Table 7. The Correlation Coefficients between the Mean Temperatures in April and October in China and the First SO Principal Components (1951–1984)

Region	Station	April	Octtober
Norrth China	Bijing	0.06	−0.52**
	Tianjin	0.01	−0.50**
	Chende	0.11	−0.45**
	Shi jiazhuang	0.11	−0.61**
	Taiyuan	0.22	−0.52**
	Hohhot	0.23	−0.37*
	Ji'nan	0.07	−0.62**
	Zhengzhou	0.06	−0.62**
	Weifang	0.03	−0.62**
	Luoyang	0.08	−0.62**
	Luohekou	0.13	−0.54**
	Xuzhou	0.12	−0.56**
Northwest China	xi'an	0.13	−0.49**
	Lanzhou	0.22	−0.31
	Tulufan	0.11	−0.36*
South China	Nanning	0.28	−0.44**
	Baise	0.23	−0.42**
	Fuzhou	0.33	−0.20
	Guangzhou	0.34*	−0.21
Northeast China	Dalian	0.13	−0.41**
	Changchun	0.05	−0.20
	Qiqihar	0.07	−0.10
	Harbin	0.11	−0.05
	Jixi	0.02	−0.21
	Shenyang	0.04	−0.37*
The middle and lower reaches of the Changjiang River and Central China	Nanjing	0.34*	−0.38*
	Shanghai	0.26	−0.26
	Hefei	0.32	−0.39*
	Anqing	0.27	−0.43**
	Hankou	0.25	−0.40*
	Hangzhou	0.26	−0.40*
	Changde	0.20	−0.39*
	Changsha	0.19	−0.24
	Ganzhou	0.36*	−0.21
	Nanchang	0.31	−0.26
Southwest China	*Kunming*	0.13	−0.10
	Guiyang	0.30	−0.10
	Chengdu	0.36*	−0.37*

* Significance level of more than 0.05.

** Significance level of more than 0.01.

2. *Warm October in the El Nino Year*

As the October polar vortex center is located in the western Hemisphere in the El Nino year and in the eastern Hemisphere or the higher latitudes of the western Hemisphere, it should be warmer in East Asia and China during the month. As shown in Table 7, all the correlation coefficients between the mean temperatures at the 38 stations in October are negative, almost half of which reach the significance level of 0.01 with those in North China most ramarkable. In addition, all the mean value differences of the temperatures at the 38 stations in October are positive. As the polar vortex center in October of the El Nino year is inclined

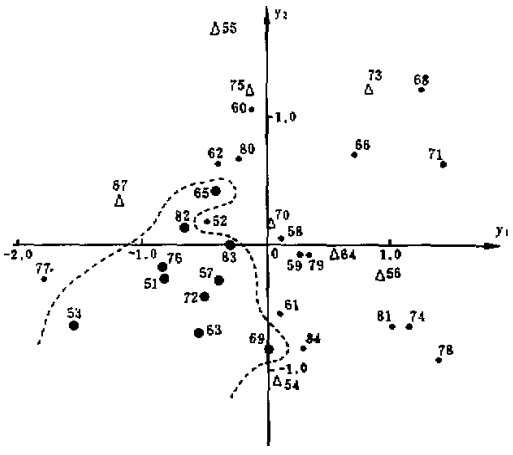

Fig.6 The two-dimensional mapped chart obtained by using the EOF expansion coefficients of the polar vortex.

to the southern latitudes of the western Hemisphere, the northern part of North America is colder and the Iceland low is deeper than in normal years.

V. STATISTICAL DIAGNOSIS FOR THE EL NINO YEARS

So far we have discussed the telecorrelation between El Nino / SO and the polar circulation with emphasis on the abnomalies of the polar circulation and weather / climate in April and October. In order to depict vividly the telecorrelation between the polar circulation and El Nino and its role in the statistical diagnosis of El Nino, the three variables listed in Table 5 (as indicated by x_1, x_2 and x_3 respectively) are nonlinearly mapped in the two-dimensional y_1 and y_2 with the definition error function as (Shi, et al., 1989):

$$K = \frac{1}{\sum_{i<j} d_{ij}^*} \sum_{i<j}^{n} \frac{(d_{ij}^* - d_{ij})^2}{d_{ij}^*} \quad , \tag{5}$$

where d_{ij}^* is the distance between point i and point j in the three-dimensional space, i.e.,

$$d_{ij}^* = \sqrt{\sum_{k=1}^{3} (x_{ki} - x_{kj})^2} \qquad (i,j = 1,2,...n) \ ,$$

where d_{ij} is the distance between point i and point j on the mapped surface (the coordinates system is y_1 o y_2), i.e.,

$$d_{ij} = \sqrt{(y_{1i} - y_{1j})^2 + (y_{2i} - y_{2j})^2} \qquad (i,j = 1,2,...n) \ .$$

The position of Samples i and j in the two-dimensional space is adjusted by the relaxation method and y_{1i} and y_{2i} obtained to all the sample points are made to have

$$K = \min \ .$$

By using the three variables in Table 5, the 34 sample points are reduced in dimension, thus obtaining the mapped chart with two-dimensional plane (Fig.6), in which the El Nino years are denoted by the blackened circles and the anti-El Nino year by triangles. By using the

EOF expansion coefficients of the three polar vortexes the El Nino phenomena can be well diagnosed.

VI. CONCLUSIONS

1. The mean polar vortex field has a characteristic regime in January and the anomaly field has a characteristic regime in April.

2. In April of the El Nino year the polar vortex is continuously split into a dipole pattern, with the 2-wave amplitude intensified. The East Asian huge trough shows persistent anomaly, causing more cold wave and cold flow activities. This situation feedbacks or intensifies the El Nino phenomenon.

3. In the year when El Nino occurs and develops, the polar vortex center in October is inclined to the westen Hemisphere. The Aleutian low is steadily deepened, and so is the Iceland low. Consequently, it is relatively warmer in China and cooler in North America.

4. There exists a good telecorrelation between El Nino / SO and the polar vortex activities. By using the EOF expansion coefficients of the polar vortex, the El Nino events can be statistically diagnosed by the nonliear mapped method.

The authors wish to express their thanks to prof. Li Chongying for his going over the manuscript and valuable comments.

REFERENCES

Cao Hongxing and Chen Guofan (1979), The application of multiple-factor composite dimension-reducing method-nonlinear mapping to weather forecasting, *Scientia Atmuspherica Sinica* 3: 158-163. (in Chinese)

Chen Xinfang, Chao Shuyi and Liu Zhongling (1986), Asummary of the polar vortex studies, *Met. Tech.* No. 3, 53-58. (in Chinese)

Dong Ming, Wei Fengying and Li Xiaoquan (1987), A trial study on the use of EOF to represent the polar height field, *Journal of the Research Institute of Meteorological Science*, Vol. 2, No. 1, 51-58.

Feng Peizhi, Li Cuijin and Li Xiaoquan (1985), *Analysis of the main meteorological disasters in China* (1951-1980), Meteorological Press. (in Chinese)

Li Chongying (1986), El Nino and typhoon activities in the South China Sea, *Tropical Met.*, Vol. 2, No. 2, 117-123. (in Chinese)

Li Chongying (1988), Erequent activities of the East Asian huge trough and occurrences of El Nino, *Scientia Sinica*, Series B, No. 6., 667-674. (in Chinese)

Shi Neng (1988), Temporal and Spatial structural characteristics of the rainfall and temperature fields during autumn and winter in China and their application to early summer precipitation prediction, *Scientia Atmospherica Sinica* 12: 283-291. (in Chinese)

Shi Neng (1989), The multiple statistical analysis of the SOI and its relation to the NH 500 hPa monthly mean circulation, *Acta Meteorologica Sinica*, 47: 457-465. (in Chinese)

Shi Neng and Chen Hui (1989), Some super long-wave characteristics in the 500 hPa monthly mean chart for the years of strong / weak SO, *Met. Sci.*, Vol. 9, No. 2, 139-147. (in Chinese)

Shi Neng, Liu Weibing and Miao Zishu (1989), The relationship between SO and the large-scale monthly / seasonal temperatures in China, *Meteor.*, 15(12), 8-12. (in Chinese).

Wang Shaowu (1985), The El Nino years in the period of 1860-1979, *Kexue Tongbao*, No. 1, 52-56. (in Chinese)